

# Polyelectrolyte Multilayers Prepared from Water-Soluble Poly(alkoxythiophene) Derivatives

Jukka Lukkari,\* Mikko Salomäki, Antti Viinikanoja, Timo Ääritalo, Janika Paukkunen, Natalia Kocharova, and Jouko Kankare

Contribution from the Department of Chemistry, University of Turku, FIN-20014 Turku, Finland

Received December 27, 2000

**Abstract:** Electronically conducting polyanion and polycation based on poly(alkoxythiophene) derivatives, poly-3-(3'-thienyloxy)propanesulfonate (P3TOPS) and poly-3-(3'-thienyloxy)propyltriethylammonium (P3TOPA) have been synthesized. Both polymers are water-soluble and exhibit high conjugation length in solution and in the solid state. These polyelectrolytes were used to prepare conducting and electroactive polyelectrolyte multilayers by the sequential layer-by-layer adsorption technique. In aqueous solutions multilayers of P3TOPS with inactive polyelectrolytes (e.g., poly(diallyldimethylammonium chloride), PDADMA) displayed electrochemical and optical behavior similar to polythiophene films prepared in organic media. Their in-plane conductivity was low (ca.  $1.6 \times 10^{-5}$  S cm<sup>-1</sup>). The conductivity could, however, be increased by a factor of ca. 40 in "all-thiophene" films, in which P3TOPA was substituted for the inactive polycation (PDADMA). The interpenetration of layers is of prime importance in films containing conducting components. The interpenetration of P3TOPS was studied by measuring the charge-transfer rate across an insulating polyelectrolyte multilayer between the substrate and the P3TOPS layer with modulated electroreflectance. The extent of interpenetration was 8–9 polyelectrolyte layers, the length scale (7–15 nm) depending on the nature of the insulating layer and, especially, on the ionic strength of the solution used for the adsorption of P3TOPS.

## Introduction

The sequential adsorption of polyanions and polycations on charged surfaces offers a simple and versatile method for the preparation of stable ultrathin multicomposite films, polyelectrolyte multilayers (PEMs).<sup>1</sup> The components are held firmly together by the multiple electrostatic interactions between the oppositely charged groups. The key to the formation of PEMs is the surface charge reversal, which takes place at every adsorption step, thus ensuring practically an unlimited number of adsorption cycles. The adsorption can be considered as a kinetically hindered equilibrium process which consists of a fast (few seconds) and a slow step.<sup>2</sup> The thickness of individual layers can be controlled by the ionic strength of the adsorption solution, higher concentrations of small electrolytes yielding thicker polyelectrolyte layers.<sup>3,4</sup> With weak polyelectrolytes, very interesting variations of the layer thickness by control of the polyelectrolyte and surface charge density with pH have been demonstrated.<sup>5</sup> Only minor amounts of small counterions

have been detected in as-prepared water-rinsed PEMs, suggesting complete intrinsic charge compensation.<sup>4,6</sup> On the other hand, exposure of the films to solutions of high salt concentration or pure water causes the uptake or expulsion of small counterions (ion breathing), and up to 30% of the ionic groups in the outer layers of PEMs are not involved in ion pair formation with the oppositely charged polyelectrolyte.<sup>7,8</sup> In addition, polyelectrolyte multilayers contain a considerable amount of water in ambient environment.<sup>4,9</sup> PEMs are not well-ordered at the molecular level and characteristically exhibit considerable interpenetration between the adjacent layers.<sup>1,4,10</sup> Due to the lack of short-range order only long-range lamellar superstructures can be constructed. However, several possible applications of PEMs as permselective membranes,<sup>11</sup> sensors,<sup>12</sup> biosensors and bioreactors,<sup>13</sup> in light-emitting diodes (LED),<sup>14</sup>

\* To whom correspondence should be addressed. Email: jukka.lukkari@utu.fi, fax: +358-2-333 6700.

(1) (a) Decher, G. *Science* **1997**, *277*, 1232–1237. (b) Bertrand, P.; Jonas, A.; Laschewsky, A.; Legras, R. *Macromol. Rapid Commun.* **2000**, *21*, 319–348.

(2) (a) Lowack, K.; Helm, C. A. *Macromolecules* **1998**, *31*, 823–833. (b) Advincula, R.; Aust, E.; Meyer, W.; Knoll, W. *Langmuir* **1996**, *12*, 3536–3540. (c) Tsukruk, V. V.; Bliznyuk, V. N.; Visser, D.; Campbell, A. L.; Bunning, T. J.; Adams, W. W. *Macromolecules* **1997**, *30*, 6615–6625. (d) McAloney, R. A.; Goh, M. C. *J. Phys. Chem. B* **1999**, *103*, 10729–10732.

(3) Decher, G.; Schmitt, J. *Prog. Colloid Polym. Sci.* **1992**, *89*, 160–164.

(4) Lösche, M.; Schmitt, J.; Decher, G.; Bouwman, W. G.; Kjaer, K. *Macromolecules* **1998**, *31*, 8893–8906.

(5) (a) Yoo, D.; Shiratori, S. S.; Rubner, M. F. *Macromolecules* **1998**, *31*, 4309–4318. (b) Shiratori, S. S.; Rubner, M. F. *Macromolecules* **2000**, *33*, 4213–4219.

(6) Schlenoff, J. B.; Ly, H.; Li, M. *J. Am. Chem. Soc.* **1998**, *120*, 7626–7634.

(7) Dubas, S. T.; Schlenoff, J. B. *Macromolecules* **1999**, *32*, 8153–8160.

(8) Caruso, F.; Lichtenfeld, H.; Donath, E.; Möhwald, H. *Macromolecules* **1999**, *32*, 2317–2328.

(9) Farhat, T.; Yassin, G.; Dubas, S. T.; Schlenoff, J. B. *Langmuir* **1999**, *15*, 6621–6623.

(10) Baur, J. W.; Rubner, M. F.; Reynolds, J. R.; Kim, S. *Langmuir* **1999**, *15*, 6460–6469.

(11) (a) Krasemann, L.; Tieke, B. *Langmuir* **2000**, *16*, 287–290. (b) Harris, J. J.; Bruening, M. L. *Langmuir* **2000**, *16*, 2006–2013.

(12) (a) Fäid, K.; Leclerc, M. *J. Am. Chem. Soc.* **1998**, *120*, 5274–5278. (b) Kumpumbu-Kalemba L., Leclerc, M. *J. Chem. Soc., Chem. Commun.* **2000**, 1847–1848.

(13) for a recent review of biologically oriented applications, see, e.g.: Lvov, Y., Möhwald, H., Eds.; *Protein Architecture. Interfacing Molecular Assemblies and Immobilization Biotechnology*; Marcel Dekker: New York, 2000.

(14) (a) Ho, P. K. H.; Granström, M.; Friend, R. H.; Greenham, N. C. *Adv. Mater.* **1998**, *10*, 769–774. (b) Ho, P. K. H.; Kim, J.-S.; Burroughes, J. H.; Becker, H.; Li, S. F. Y.; Brown, T. M.; Cacialli, F.; Friend, R. H. *Nature* **2000**, *404*, 481–484.

and in preparation of micrometer-scale hollow systems<sup>15</sup> have been suggested.

Most of the work on PEMs has been carried out using nonconjugated polyelectrolytes. Less attention has been given to functional, for example, electroactive polyelectrolytes such as polyviologens.<sup>16</sup> Electronically conducting multilayers have been prepared by using oxidized polyaniline and polypyrrole as polycations.<sup>17</sup> Owing to their special electrical and optical properties mono- and multilayers prepared from conducting polyelectrolytes should be interesting materials for potential applications in the fields of sensors, electrooptics, and LED technology.<sup>1,12,14</sup> Conducting polymers carrying ionic substituents are permanently charged polyelectrolytes, so-called self-doped conducting polymers.<sup>18</sup> An attractive feature of the use of self-doped conducting polymers is the possibility to form a uniform conducting coating on any charged substrate with precise control of the thickness, irrespective of form or size of the substrate, by simply dipping it into an aqueous polymer solution. There are only few papers dealing with the fabrication and properties of multilayers prepared from ionically substituted conducting polymers. Rubner et al. were the first to demonstrate that ultrathin conducting layers can be fabricated using carboxylic acid-derivatized polythiophenes.<sup>19</sup> Light-emitting diodes have been prepared by sequential adsorption of anionic and cationic poly(*p*-phenylene)s.<sup>20</sup> We have recently shown that multilayers can be prepared from sulfonated poly(alkoxythiophene) and that the linear charge density of the conducting polymer, that is, its oxidation state, affects the multilayer formation.<sup>21</sup> The use of alkoxy-substituted thiophenes is advantageous over alkyl derivatives because oxygen is sterically less demanding than the methylene group.<sup>22</sup> Careful attention to the head-to-tail (HT) coupling is, therefore, not so important, and simple oxidative polymerization methods can be used although the conductivities of the resulting materials are generally low. In addition, oxygen directly attached to the thiophene ring lowers the oxidation potential of the monomer and polymer, which is beneficial for work in aqueous medium.<sup>23</sup> In this work we describe the electrochemical and optical behavior of polyelectrolyte multilayers prepared using a conducting poly-3-(3'-thienyloxy)propanesulfonate (P3TOPS, Scheme 1). We also give the first report on all-thiophene polyelectro-

(15) Donath, E.; Sukhorukov, G. B.; Caruso, F.; Dacis, S.; Möhwald, H. *Angew. Chem., Int. Ed.* **1998**, *37*, 2201–2205.

(16) (a) Laurent, D.; Schlenoff, J. B. *Langmuir* **1997**, *13*, 1552–1557. (b) Schlenoff, J. B.; Laurent, D.; Ly, H.; Stepp, J. *Adv. Mater.* **1998**, *10*, 347–349. (c) Stepp, J.; Schlenoff, J. B. *J. Electrochem. Soc.* **1997**, *144*, L155–L157.

(17) (a) Cheung, J. H.; Fou, A. F.; Rubner, M. F. *Thin Solid Films* **1994**, *244*, 985–989. (b) Fou, A. C.; Rubner, M. F. *Macromolecules* **1995**, *28*, 7115–7120. (c) Cheung, J. H.; Stockton, W. B.; Rubner, M. F. *Macromolecules* **1997**, *30*, 2712–2716. (d) Stockton, W. B.; Rubner, M. F. *Macromolecules* **1997**, *30*, 2717–2725. (e) Ram, M. K.; Salerno, M.; Adami, M.; Faraci, P.; Nicolini, C. *Langmuir* **1999**, *15*, 1252–1259.

(18) (a) Chayer, M.; Faïd, K.; Leclerc, M. *Chem. Mater.* **1997**, *9*, 2902–2905. (b) McCullough, R. D.; Ewbank, P. C.; Loewe, R. S. *J. Am. Chem. Soc.* **1997**, *119*, 633–634. (c) Arroyo-Villan, M. I.; Diaz-Quijada, G. A.; Abdou, M. S. A.; Holdcroft, S. *Macromolecules* **1995**, *28*, 975–984.

(19) (a) Cheung, J. H.; Fou, A. F.; Ferreira, M.; Rubner, M. F. *Polym. Prepr.* **1993**, *34*, 757–758. (b) Ferreira, M.; Cheung, J. H.; Rubner, M. F. *Thin Solid Films* **1994**, *244*, 806–809. (c) Fou, A. C.; Onitsuka, O.; Ferreira, M.; Rubner, M. F. *Mater. Res. Soc. Symp. Proc.* **1995**, *369*, 575–580. (d) Ferreira, M.; Rubner, M. F. *Macromolecules* **1995**, *28*, 7107–7114.

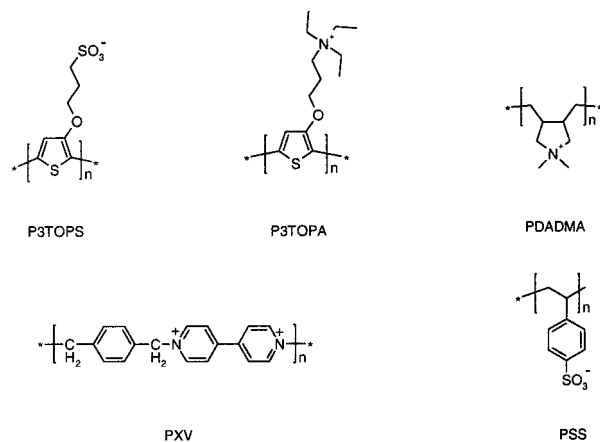
(20) Baur, J. W.; Kim, S.; Balanda, P. B.; Reynolds, J. R.; Rubner, M. F. *Adv. Mater.* **1998**, *10*, 1452–1455.

(21) Lukkari, J.; Viinikanoja, A.; Paukkunen, J.; Salomäki, M.; Janhonen, M.; Äärtilo, T.; Kankare, J. *J. Chem. Soc., Chem. Commun.* **2000**, 571–572.

(22) (a) Meille, S. V.; Farina, A.; Bezziccheri, F.; Gallazzi, M. C. *Adv. Mater.* **1994**, *6*, 848–851. (b) Faïd, K.; Cloutier, R.; Leclerc, M. *Macromolecules* **1993**, *26*, 2501–2507.

(23) Leclerc, M.; Faïd, K. *Adv. Mater.* **1997**, *9*, 1087–1094.

### Scheme 1. Structures of the Polyelectrolytes Used in the Present Study



lyte multilayers containing P3TOPS and a cationic polythiophene derivative, poly-3-(3'-thienyloxy)propyltriethylammonium (P3TOPA, Scheme 1), as polyanion and polycation, respectively. In addition, we address the interpenetration of polyelectrolyte layers by using the charge-transfer rate between the conducting polymer and the substrate surface as a probe for the penetration of polythiophene into the film.

### Experimental Section

**Materials.** Deuterium oxide (D<sub>2</sub>O, Aldrich), 2-mercaptoethanesulfonic acid (MESA, Aldrich), 2-aminoethanethiol hydrochloride (MEA, Aldrich), *N*-(trimethoxysilylpropyl)-*N,N,N*-trimethylammonium chloride (TMSPA from ABCR, Germany), (3-aminopropyl)diethoxymethylsilane (Fluka), and (3-aminopropyl)triethoxysilane (ICN Biochemicals) were used as received. All aqueous solutions were prepared in 18 MΩ cm water (Millipore). Poly(diallyldimethylammonium chloride) (PDADMA), *M<sub>w</sub>* = 400 000–500 000, and poly(sodium 4-styrenesulfonate) (PSS), *M<sub>w</sub>* = 70 000, were purchased from Aldrich and used as received. Poly(*p*-xylyleneviologen bromide) (PXV) was synthesized as described in the literature and dialyzed using a membrane with a nominal molecular weight cutoff of 3500.<sup>24</sup>

**Sodium 3-(3'-Thienyloxy)propanesulfonate.** 3-(3-Bromo)propoxythiophene was synthesized from 3-methoxythiophene and 3-bromopropanol analogously as described in ref 18a for 2-bromoethanol. <sup>1</sup>H NMR (CDCl<sub>3</sub>, 400 MHz, ppm): 7.18 (1H, dd), 6.75 (1H, dd), 6.27 (1H, dd), 4.10 (2H, t), 3.58 (2H, t), 2.30 (2H, td). The product was refluxed with Na<sub>2</sub>SO<sub>3</sub> in acetone/water (2:1), evaporated to dryness, and the crude product dissolved in ethanol. Recrystallization from ethanol yielded white crystals of sodium 3-(3'-thienyloxy)propanesulfonate. <sup>1</sup>H NMR (D<sub>2</sub>O, 400 MHz, ppm): 7.36 (1H, dd), 6.85 (1H, dd), 6.57 (1H, dd), 4.17 (2H, t), 3.08 (2H, m), 2.21 (2H, m). <sup>13</sup>C NMR (400 MHz): 157.2, 126.4, 119.9, 99.9, 69.5, 48.5, 24.9 (see Supporting Information for the NMR spectra).

**3-(3'-Thienyloxy)propyltriethylammonium Bromide.** Triethylamine (23.5 mmol) was added to a solution (10 mL) of 3-(3-bromo)propoxythiophene (5.88 mmol) in ethanol. The mixture was refluxed for 72 h and evaporated to dryness. The product was let to crystallize overnight in diethyl ether (yield 96%). <sup>1</sup>H NMR (hexafluorophosphate salt, DMSO, 400 MHz, ppm): 7.43 (1H, dd), 6.76 (1H, dd), 6.60 (1H, m), 4.02 (2H, t), 3.23 (8H, m), 2.05 (2H, m), 1.17 (9H, t). <sup>13</sup>C NMR (400 MHz): 156.8, 125.7, 119.3, 98.5, 66.6, 53.3, 52.0, 21.3, 7.1 (see Supporting Information for the NMR spectra).

**Polymerization.** The polymerizations were carried out with anhydrous FeCl<sub>3</sub> (mole ratio ca. 4:1) in dry CHCl<sub>3</sub>.<sup>18a</sup> With sodium 3-(3'-thienyloxy)propanesulfonate the mixture was filtered after 3 days and the polymer dissolved in 2 M NaOH/10% hydrazine. Iron hydroxide was removed by centrifugation. The neutralized crude polymer solution was dialyzed against water for 2 days (using a 3500 nominal molecular

(24) Factor, A.; Heinsohn, G. E. *Polym. Lett.* **1971**, *9*, 289–295.

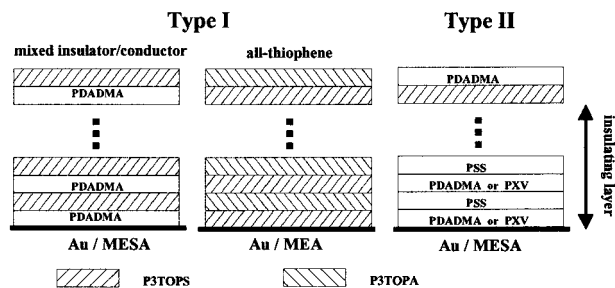
weight cutoff membrane). After concentration the solution was fractionated with a Sephadex G-50 F column using water as eluent and the high-molecular weight fraction collected. This fraction was concentrated, and some NaOH and hydrazine were added under nitrogen atmosphere in order to ensure conversion to the neutral sodium salt. Ethanol was added to precipitate poly-3-(3'-thienyloxy)propanesulfonate (P3TOPS) and polymer was finally washed with ethanol. The final iron content was below 500 ppm as determined by inductively coupled plasma mass spectrometry (ICP-MS). Before the polymerization of 3-(3'-thienyloxy)propyltriethylammonium bromide the anion was first replaced with hexafluorophosphate using an anion-exchange resin. The oxidative polymerization was carried out as described above for a period of 2 weeks. The crude polymer was separated and dialyzed similarly and used without fractionation.

**Polymer Characterization.** The polymers were characterized in solution by UV-vis spectroscopy using a Hewlett-Packard 8453 spectrophotometer. Raman spectra were obtained by Nexus 870 FT-IR equipped with a FT-Raman module (Nicolet) from aqueous polymer solutions that were 10 mM with respect to the monomers. The Raman excitation wavelength was 1064 nm. The spectra were characteristic for polythiophenes (see Supporting Information for the spectra and the assignments of the major bands). The average molecular weight of P3TOPS was estimated by size-exclusion chromatography (SEC) in a DMSO/H<sub>2</sub>O solvent mixture (96:4 v/v) at 70 °C with a PLgel mixed bed column (Agilent Technologies) using sodium poly(styrene sulfonate) standards (Polymer Standards Service, Germany). The eluent contained 0.03 M KPF<sub>6</sub>.

**Preparation of Multilayers.** The thin-film Au electrodes were prepared on either Si(100) wafers (for electrochemistry and electroreflectance) or microscope glass slides (for conductivity measurements). Silicon wafers and glass slides were first cleaned in concentrated H<sub>2</sub>SO<sub>4</sub>/30% H<sub>2</sub>O<sub>2</sub> (3:1) ("piranha" solution; warning: piranha solution is very corrosive and must be treated with extreme caution; it reacts violently with organic material and must not be stored in tightly closed vessels), rinsed thoroughly with Millipore water, and dried. The silicon substrates were then silanized with (3-aminopropyl)triethoxysilane in dry toluene solution (1% v/v) for 4 min at 60 °C and the glass substrates were silanized by using (3-aminopropyl)diethoxymethylsilane (1–2 h at room temperature).<sup>25</sup> A thin gold layer (ca. 100 nm) was then formed by resistive thermal evaporation using an Edwards E306A coating system. The charging of the gold surface required for polyelectrolyte adsorption was effected by chemisorption of a self-assembled monolayer of MESA or MEA for negatively or positively charged surfaces, respectively. The tin oxide-coated glass electrodes were cleaned similarly, and their surfaces were charged positively with TMSPA.<sup>26</sup> Polyelectrolyte adsorption was carried out using 10 mM (with respect to monomer) PDADMA or PSS solutions and 1 mM P3TOPS, P3TOPA, and PXV solutions in water. The adsorption time was 30 min for P3TOPS and P3TOPA and 15 min for the other polyelectrolytes. The ionic strength was adjusted either by Na<sub>2</sub>SO<sub>4</sub> (oxidized P3TOPS) or Na<sub>2</sub>S<sub>2</sub>O<sub>4</sub> (neutral P3TOPS) and was 0.6 M unless otherwise stated. Between every adsorption step the surface was rinsed 3 × 1 min in clean water after first rinsing it with running Millipore water and finally dried. Two types of multilayers were studied in the present work (Scheme 2). Type I films consisted of successively adsorbed layers of P3TOPS and a nonelectroactive polycation (usually PDADMA) or P3TOPA (all-thiophene multilayers). In type II films a single P3TOPS layer was separated from the electrode surface by a number of inactive spacer layers (PDADMA, PSS, PXV). The conducting layer was capped by a layer of PDADMA for increased stability.<sup>27</sup>

**Multilayer Characterization.** The experimental setup used in the modulated electroreflectance measurements has been reported elsewhere.<sup>28</sup> A small ac potential modulation (amplitude 14 mV) was used

**Scheme 2.** Idealized Structures of Type I and Type II Polyelectrolyte Multilayers



for excitation and the resulting ac variation of the electrode surface reflectance ( $\Delta R_{ac}$ ) measured. The signal was normalized with the measured ac potential across the interface and the dc-reflectance ( $R$ ) to give  $1/R (dR/dE)$ . All reflectance measurements were carried out at 600 nm. Electrochemical measurements were performed in a three-electrode one-compartment cell using either EG&G 283 or 263A potentiostats. All potentials are referred to the aqueous saturated calomel electrode (SCE). All solutions were degassed with argon before measurements. In situ UV-visible and NIR spectra were measured in D<sub>2</sub>O using spectrometers described above. The quartz crystal microbalance (QCM) measurements were performed with 10 MHz AT-cut crystals using a Seiko QCA917 analyzer. The gold-plated crystals were primed with MESA, and the frequency shift was measured after different steps with the loaded side of the crystal in contact with pure water. Assuming rigid layer behavior the frequency changes  $\Delta f$  can be converted to mass loadings using the Sauerbrey equation:<sup>29</sup>

$$\Delta f = - \frac{2f_0^2}{A(\mu_q \rho_q)^{1/2}} \Delta m \quad (1)$$

Here  $f_0$  is the fundamental resonance frequency of the crystal,  $A$  the electrode area,  $\mu_q$  and  $\rho_q$  the shear modulus and density of quartz, respectively. The thickness of PDADMA/PSS and PXV/PSS multilayers was determined on a Sentech SE 400 ellipsometer operating at 632.8 nm and using an effective refractive index 1.47 for the polymer films.<sup>8,16a</sup> Multilayer conductivity was determined by a four lead method by using four identical gold electrodes evaporated on glass. The film was withdrawn from an electrochemical cell in an oxidized state (+0.6 V vs SCE), rinsed, dried, and transferred into a glovebox. The conductance was measured on a Keithley 2400 SourceMeter in dry (H<sub>2</sub>O < 5 ppm, O<sub>2</sub> < 1 ppm) nitrogen atmosphere. The thickness of multilayers on silanized glass was measured with atomic force microscopy (AFM) in at least 10 different positions. The film thickness values used in the conductivity calculations were  $23.3 \pm 2.5$  nm and  $17.5 \pm 1.5$  nm for the (P3TOPS/PDADMA)<sub>5</sub> and (P3TOPS/P3TOPA)<sub>5</sub> multilayers, respectively. All experiments were carried out at room temperature.

## Results and Discussion

**Polymer Characterization.** Both polythiophene derivatives, poly-3-(3'-thienyloxy)propanesulfonate (P3TOPS) and poly-3-(3'-thienyloxy)propyltriethylammonium (P3TOPA), showed good solubility in water and some organic solvents, such as methanol and dimethyl sulfoxide (DMSO). The absorbance maximum of neutral P3TOPS in water was at 615 nm, but high absorbance was observed also at longer wavelengths (see Supporting Information for the UV-vis spectra) and was attributed to scattering due to aggregation or to residual oxidized segments. Polythiophenes are known to aggregate in poor solvents, and aggregate formation has been demonstrated also for sulfonated poly(*p*-phenylene)s in water.<sup>30,31</sup> In DMSO the  $\pi \rightarrow \pi^*$  transition

(29) Sauerbrey, G. Z. *Phys.* **1959**, *155*, 206.

(30) Kilbinger, A. F. M.; Feast, W. J. *J. Mater. Chem.* **2000**, *10*, 1777–1784.

(25) Moon, J. H.; Shin, J. W.; Kim, S. Y.; Park, J. W. *Langmuir* **1996**, *12*, 4621–4624.

(26) Szentirmay, M. N.; Campbell, L. F.; Martin, C. R. *Anal. Chem.* **1986**, *58*, 661–662.

(27) Hoogeveen, N. G.; Cohen Stuart, M. A.; Fleer, G. J. *Langmuir* **1996**, *12*, 3675–3681.

(28) Lukkari, J.; Kleemola, K.; Meretoja, M.; Ollonqvist, T.; Kankare, J. *Langmuir* **1998**, *14*, 1705–1715.

displayed a blue-shift to 600 nm, and absorption at longer wavelengths disappeared. The absorption maximum of P3TOPA was 582 nm in water and DMSO. Compared to other poly-(alkoxythiophene)s the absorbance maxima are at low energy, indicating a high conjugation length for both polymers.<sup>18a,22b</sup> In PDADMA/P3TOPS and P3TOPA/PSS multilayers the absorption maxima were at 630 and 580 nm, respectively. Because of possible aggregation the SEC characterization of P3TOPS was carried out in DMSO containing 4% of water (we were unable to determine the molecular weights with aqueous SEC).<sup>21</sup> For several different preparation lots the measurements showed a number-average molecular weight of ca. 6000–10 000 with a polydispersity index of 2.5–2.9. This molecular weight is similar to those reported for other water-soluble poly(alkoxythiophene)s and implies an average chain length of ca. 30–40 monomer units. It should be born in mind, however, that SEC has been shown to exaggerate polythiophene molecular weights, mainly because of the lack of suitable standards for rigid polythiophenes.<sup>32</sup> An attempt was also made to determine the molecular weight of P3TOPA using SEC and water- or organic-based columns in various water–organic mixtures but with no success. The efforts to use matrix assisted laser desorption ionization time-of-flight (MALDI-TOF) technique for P3TOPS or P3TOPA were not successful either.

**Multilayer Formation.** The charge density of the surface and that of a weak polyelectrolyte exhibits a strong effect on the formation of polyelectrolyte multilayers.<sup>5</sup> With P3TOPS, the charge density can be adjusted by controlling the oxidation state of the polymer, analogous to the pH control in the case of weak polyelectrolytes.<sup>21</sup> In aqueous solutions, P3TOPS is stable in the oxidized form and can be kept in the neutral form (referring to the polymer backbone) only in the presence of strong reductants, such as hydrazine or sodium dithionite. To determine the suitable conditions for multilayer preparation we have studied the effect of P3TOPS charge density using a quartz crystal microbalance (Figure 1). First, both polyelectrolytes (oxidized P3TOPS and PDADMA) were adsorbed from 0.2 M Na<sub>2</sub>SO<sub>4</sub> solutions. Second, 0.2 M Na<sub>2</sub>S<sub>2</sub>O<sub>4</sub> solutions were used to keep the adsorbing and adsorbed P3TOPS in the neutral state. Rinsing between the layers was accomplished either with oxygen- or nitrogen-saturated water. Assuming rigid film behavior (previous studies on polyelectrolyte multilayers suggest that QCM data can be treated in a gravimetric manner),<sup>33</sup> the average mass increment is ca. 1.3 and 2.6  $\mu\text{g cm}^{-2}$ /bilayer for the first and second case, respectively (including an unknown contribution from water). After a few initial layers a regular zigzag behavior is observed. The mass increases upon adsorption of PDADMA on neutral P3TOPS but decreases (or does not change appreciably) upon adsorption of neutral P3TOPS on PDADMA. On the other hand, the mass increases upon adsorption of oxidized P3TOPS but stays nearly constant after PDADMA adsorption. Similar zigzag behavior has been reported in the adsorption of low charge density polyelectrolytes.<sup>27,34</sup> While a definite explanation for these observations cannot be given, they can be tentatively connected to the poorer adhesion due to a lower charge density. However, the results imply that the use of oxidized P3TOPS results in greater relative

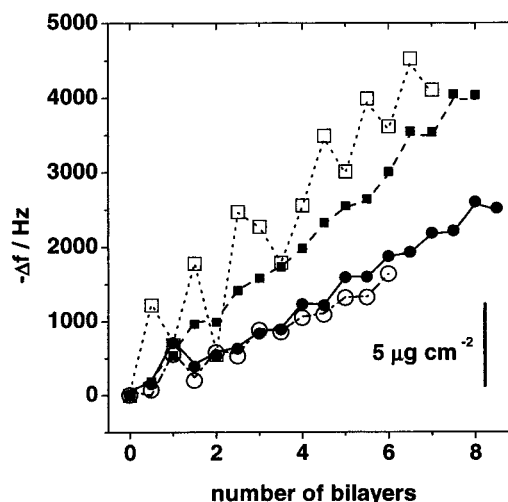


**Figure 1.** QCM frequency changes upon sequential adsorption of P3TOPS and PDADMA from solutions containing 0.2 M Na<sub>2</sub>SO<sub>4</sub> or Na<sub>2</sub>S<sub>2</sub>O<sub>4</sub>. Symbols: (□) neutral, and (●) oxidized P3TOPS; (■) oxidized P3TOPS on PDADMA, PDADMA on neutral P3TOPS; (○) neutral P3TOPS on PDADMA, PDADMA on oxidized P3TOPS (see text for explanations). Whole numbers in the abscissa correspond to P3TOPS as outmost layer. The bar corresponds to a mass loading of 5  $\mu\text{g cm}^{-2}$  (calculated from eq 1 assuming rigid film behavior). The lines shown are guides to the eye.

amount of electroactive material although the total amount of adsorbed polyelectrolyte is higher in the other case. This conclusion is supported by the electrochemical measurements (vide infra).

We have also prepared multilayers by adsorbing successively neutral P3TOPS on PDADMA and PDADMA on oxidized P3TOPS (using oxygen-saturated Na<sub>2</sub>SO<sub>4</sub> solutions), or oxidized P3TOPS on PDADMA and PDADMA on neutral P3TOPS (using Na<sub>2</sub>S<sub>2</sub>O<sub>4</sub> solutions). The average mass increments were ca. 1.1 and 2.0  $\mu\text{g cm}^{-2}$ /bilayer, respectively. However, the behavior in these mixed cases was more ambiguous and was not analyzed further. In conclusion, these experiments show that although the charge density of P3TOPS affects the film formation multilayers can be prepared irrespective of its oxidation state. To simplify the chemistry during multilayer fabrication we have chosen to use exclusively the oxidized form of P3TOPS in the following work unless otherwise stated.

**Characterization of Type I Multilayers. Electrical Properties.** Electroactive multilayers can be formed by sequential adsorption of P3TOPS, and an inactive polycation, for example, PDADMA, on gold electrodes primed with a self-assembled monolayer of MESA or MEA. The electroactivity of the multilayers can be attributed to the interpenetration of the electroactive and inactive layers. The peak currents increase linearly after 3–4 bilayers (Figure 2), being higher for multilayers prepared from oxidized P3TOPS than the neutral form of the polymer, which supports the QCM observations that more electroactive material is adsorbed in the former case. In general, the electrochemical behavior of PDADMA/P3TOPS multilayers in aqueous solutions is similar to that of polythiophene films prepared and measured in organic media. The voltammograms exhibit typical hysteresis showing at least two oxidation processes and a broad reduction peak. The oxidation peak shifts to more anodic potentials with increasing number of layers and stabilizes at ca. +0.25 V. The shift can be attributed to slower charge-transfer kinetics in thicker films.<sup>17e</sup> The electrical in-plane conductivity of a (PDADMA/P3TOPS)<sub>5</sub> film was measured using a four-lead method and was 1.6 ×

(31) Rulkens, R.; Wegner, G.; Thurn-Albrecht, T. *Langmuir* **1999**, *15*, 4022–4025.

(32) Liu, J.; Loewe, R. S.; McCullough, R. D. *Macromolecules* **1999**, *32*, 5777–5785.

(33) Caruso, F.; Niikura, K.; Furlong, D. N.; Okahata, Y. *Langmuir* **1997**, *13*, 3422–3426.

(34) Kolarik, L.; Furlong, D. N.; Joy, H.; Struijk, C.; Rowe, R. *Langmuir* **1999**, *15*, 8265–8275.

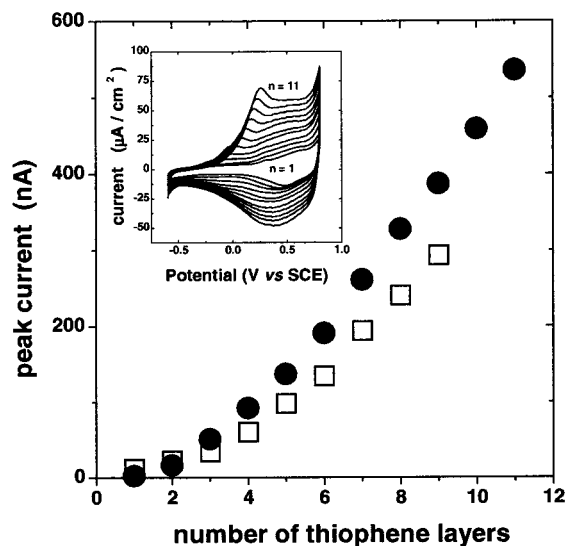


**Figure 2.** The evolution of the first oxidation peak current as a function of the number of thiophene layers assembled using PDADMA and oxidized (●) or neutral (□) P3TOPS. The inset shows the cyclic voltammograms (100 mV/s) of a Au/MESA/(PDADMA/P3TOPS)<sub>n</sub> multilayer in 0.2 M Na<sub>2</sub>SO<sub>4</sub> (assembled in 0.2 M Na<sub>2</sub>SO<sub>4</sub> using oxidized polymer; neutral polymer behaved analogously). Number of thiophene layers indicated in figure.

$10^{-5}$  S cm<sup>-1</sup>. Although the conductivities of poly(alkoxythiophene)s are generally rather low, this value is considerably smaller than that reported for macroscopic samples of similar water-soluble polymers.<sup>18a</sup> With in situ polymerized polypyrrole films Rubner et al. have shown that conducting polymer films of similar thickness are enough to attain macroscopic conductivity of the material.<sup>17b</sup> In a previous report, however, similar low-conductivity values were found for a polyelectrolyte multilayer containing PDADMA and a polythiophene derivative.<sup>35</sup> We attribute the low conductivity partly to the insulating PDADMA layers between the conducting ones. Electroreflectance measurements (vide infra) have shown that the insertion of a single PDADMA layer between the electrode and P3TOPS significantly decreases the charge-transfer rate. The conductivity could be increased by a factor of ca. 40 when PDADMA was replaced by a conducting polycation, P3TOPA ( $6.2 \times 10^{-4}$  S cm<sup>-1</sup> for (P3TOPS/P3TOPA)<sub>5</sub>), supporting this conclusion. This is a novel type of film, an all-thiophene polyelectrolyte multilayer, and it emphasizes that good contacts between the conducting layers are important for obtaining higher conductivity. Twists and other defects can also contribute to the low conductivity in these very thin polymer layers.

**Optical Properties.** The spectral evolution of PDADMA/P3TOPS multilayers during oxidation in water also displayed features characteristic for polythiophene films (Figure 3). Upon oxidation the  $\pi \rightarrow \pi^*$  transition at 630 nm decreases with a slight blue-shift (to 625 nm at potentials positive of +0.3 V), and new bands appear at ca. 820–1050 and 1870 nm. The latter band starts to shift toward higher energy at potentials positive of +0.3 V, finally reaching 1720 nm at +0.60 V. The behavior in the medium spectral range (800–1100 nm) is more complex due to at least two unresolved transitions. In this range, the difference spectra display a maximum at ca. 1000 nm at potentials below -0.2 V, whereas at higher potentials the absorbance starts to increase at ca. 850 nm. After +0.3 V a decrease in absorbance is observed, and the principal band shifts

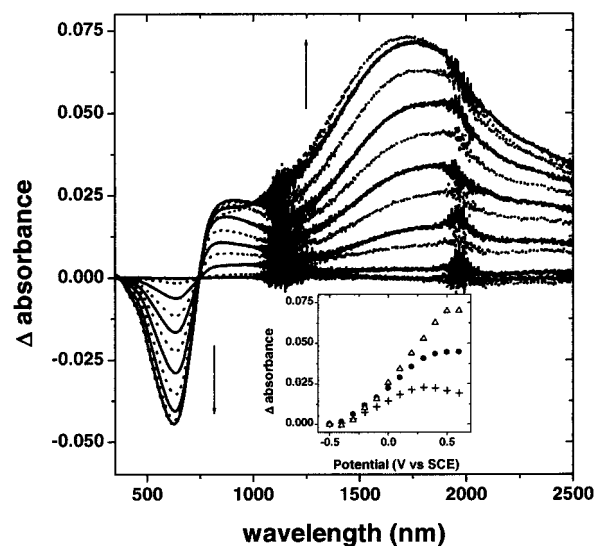


**Figure 3.** Differential absorption spectra of a SnO<sub>2</sub>/TMSPA/(P3TOPS/PDADMA)<sub>5</sub> multilayer in 0.1 M NaNO<sub>3</sub>/D<sub>2</sub>O. Spectra taken at 0.100 V intervals from -0.50 V to +0.60 V (spectrum at -0.60 V taken as reference). The inset shows the evolution of absorbance at 630 (●), 850 (+), and 1850 nm (△). Noise around 1100 and 2000 nm due to low intensity of the light sources (change from UV-vis to IR spectrometer) and strong D<sub>2</sub>O (H<sub>2</sub>O) overtones, respectively.

to ca. 900 nm. This spectral behavior is in accordance with the generation of polarons, dimerized polarons, and bipolarons as charge carriers upon doping.<sup>36</sup>

#### Study of Layer Interpenetration: Type II Multilayers.

Extensive interpenetration of adjacent polyelectrolyte layers is an inherent property of these multilayer systems, and information about the extent of interpenetration is important for the generation of layered superstructures.<sup>37</sup> X-ray and neutron reflectometry measurements of PAH/PSS multilayers have shown that a single layer overlaps approximately over four adjacent layers on both sides.<sup>2a,4</sup> The new polyelectrolyte layer can, therefore, interact with material seven to eight layers below the film surface.<sup>8</sup> In these cases, the physical extent of interpenetration is approximately 7–15 nm.

Especially, in multilayers containing polyelectrolytes capable of electron- or energy transport it is of prime importance to know how thick the separating layers have to be when inserted between the substrate surface and the active layer or two active layers to prevent short circuiting the two. Studies of Förster energy transfer between poly(*p*-phenylene vinylene) (PPV) and sulfonated poly(*p*-phenylene) (PPP) have shown that the conjugated polyelectrolytes penetrate 1–2.5 PMA/PAH bilayers (PMA = poly(methacrylic acid); this corresponds to 1.5–5.3 nm depending on adsorption conditions).<sup>10</sup> On the other hand, one thick (>5.7 nm) bilayer of PAA/PAH could separate the conjugated layers, but even eight thin PSS/PAH bilayers (total thickness over 5.3 nm) were not enough for total insulation. This demonstrates that the nature of the separating layers may have an important role. With redox active multilayers consisting of poly(butyleneviologen) (PBV) four PAH/PSS bilayers were needed to insulate the PBV layer from the electrode surface.<sup>16a</sup> To probe the interpenetration of P3TOPS during adsorption we have prepared type II multilayers in which a single layer of P3TOPS was adsorbed on top of an insulating multilayer (either PDADMA/PSS or PXV/PSS) of varying thickness (Scheme 2).

(36) Faïd, K.; Leclerc, M.; Nguyen, M.; Diaz, A. *Macromolecules* **1995**, *28*, 284–287.

(37) Hong, H.; Steitz, R.; Kirstein, S.; Davidov, D. *Adv. Mater.* **1998**, *10*, 1104–1108.

(35) Kim, J.; Wang, H.-C.; Kumar, J.; Tripathy, S. K.; Chittibabu, K., G.; Cazeca, M. J.; Kim, W. *Chem. Mater.* **1999**, *11*, 2250–2256.

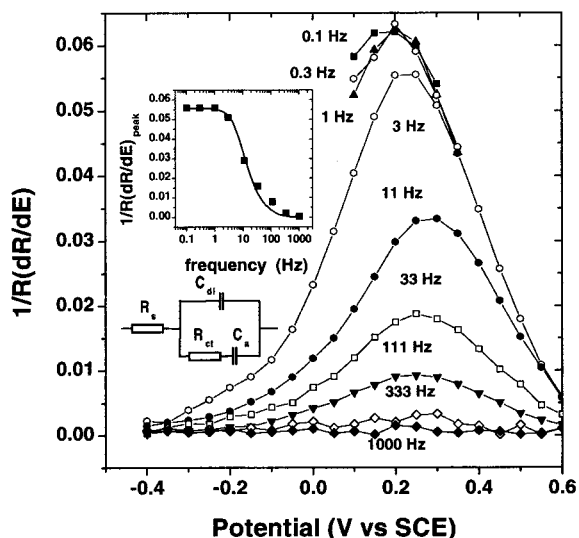


**Figure 4.** Steady-state electroreflectograms (measured at 600 nm) of a Au/MESA/PDADMA/PSS/PDADMA/P3TOPS/PDADMA multilayer in 0.2 M Na<sub>2</sub>SO<sub>4</sub>. The excitation frequencies indicated in the figure. At frequencies below 1 Hz only the central part of the curves was measured in order to decrease the measurement time. The insert shows a fit to the data according to the equivalent circuit shown ( $R_{ct}$  = charge-transfer resistance,  $C_a$  = pseudocapacitance,  $C_{dl}$  = interfacial capacitance,  $R_s$  = uncompensated solution resistance). See text for explanations.

**Charge Transfer Through Insulating Layers.** In polyelectrolyte multilayers containing electroactive polyions, the charge-transfer rate between the electrode surface and polymer would be a measure of the extent of interpenetration toward the substrate. In general, the ac techniques are better suited than simple voltammetry for precise measurement of charge-transfer rates.<sup>38</sup> An elegant method for the determination of the charge-transfer rate in an electroactive self-assembled monolayer has recently been proposed by Creager et al.<sup>39</sup> In their method ac voltammograms were measured at various excitation frequencies, and the peak values as a function of frequency were fitted to a simple equivalent circuit (see Figure 4). A single layer of P3TOPS could easily be detected on gold by ac voltammetry and square wave voltammetry (SQW), but the analysis was complicated by the nonideal, sloping background current in both cases. This stems from the fact that non-Faradaic processes contribute to the measured current, too. Spectroelectrochemical techniques provide a method for discriminating against non-Faradaic processes, and the analysis of reflectoimpedance data in the complex plane has been shown to be an effective method for the determination of electron-transfer kinetics at interfaces.<sup>40</sup> We have adopted a combination of these two methods for the analysis of the charge-transfer rate across the insulating film in type II multilayers. The steady-state electroreflectograms, that is the magnitude of an ac reflectance signal  $1/R(dR/dE)$  as a function of potential, display a nearly ideal background at different measurement frequencies (Figure 4). The small constant background is attributed to the electroreflectance signal of gold itself and can be easily subtracted. The reflectance signal originates from the reversible changes in the oxidation state of the single layer of P3TOPS on top of the insulating film. The response curve has a sigmoidal shape as a function of frequency

(38) Bard, A. J.; Faulkner, L. R. *Electrochemical Methods. Fundamentals and Applications*, 2nd ed.; John Wiley & Sons: New York, 2001; Chapter 10.

(39) Creager, S. E.; Wooster, T. T. *Anal. Chem.* **1998**, *70*, 4257–4263.

(40) Feng, Z. Q.; Sagara, T.; Niki, K. *Anal. Chem.* **1995**, *67*, 3564–3570.

(inset of Figure 4) because of finite charge-transfer rate. The magnitude of the reflectance  $Y$  (defined analogously to ac admittance as  $\Delta R_{ac} = Y\Delta E_{ac}$ , where  $\Delta R_{ac}$  and  $\Delta E_{ac}$  are the magnitudes of the reflectance change and interfacial potential excitation, respectively) can be written as

$$Y = \frac{KC_a}{[(1 - \omega^2 R_s R_{ct} C_a C_{dl})^2 + \omega^2 (R_{ct} C_a + R_s C_a + R_s C_{dl})^2]^{1/2}} \quad (2)$$

where  $\omega$  is the angular frequency,  $K$  a proportionality factor,  $R_s$ ,  $R_{ct}$ ,  $C_{dl}$ , and  $C_a$  (see Figure 4) the uncompensated solution resistance, charge-transfer resistance, double-layer capacitance, and adsorption pseudocapacitance, respectively.<sup>40</sup> At the peak potential we have for the charge-transfer rate constant  $k_{ct}$ <sup>41</sup>

$$k_{ct} = (2R_{ct} C_a)^{-1} \quad (3)$$

The charge-transfer rate can be obtained from a fit of reflectance data to eqs 2 and 3 with some chosen value for the proportionality constant.<sup>42</sup> The solution resistance and interfacial capacitance can usually be determined by ac impedance with good accuracy. An example of the fit is shown in Figure 4. A small deviation at high frequencies has been attributed by Creager et al. to the presence of fast reaction sites in the SAM. We think that in this case the deviation originates from the failure of the simple equivalent circuit to accurately describe the behavior of conducting polymer films over all frequencies used. Our own ac impedance measurements (not shown) have demonstrated that the best description of oxidized type I or type II multilayers is obtained by including a finite diffusion element in the equivalent circuit. However, it approaches an RC-circuit at low frequencies and would complicate the analysis considerably without adding any new physical insight. Therefore, we use the simple circuit as the first approximation in this work, where we are interested in the changes of the charge-transfer rate. In addition, as can be seen in Figure 5, the deviation is usually much smaller.

As the number of insulating PDADMA/PSS layers between the gold electrode and the P3TOPS layer increases, the sigmoidal reflectance curves shift to lower frequencies, indicating a decrease in the charge-transfer rate (Figure 5). The frequency shift is relatively large, 3–4 orders of magnitude when going from zero (Au/MEA/P3TOPS) to seven insulating layers. If the polythiophene layer was separated from the surface by nine layers, no signal was observed (down to the excitation frequency of 1 mHz, which is the practical lower limit of our measurement system), suggesting the complete break of the connection between the surface and P3TOPS. The rate constants obtained from the fits in Figure 5 are shown in Figure 6 as the function of the insulating layer thickness for this case, in which all the layers were assembled from solutions containing 0.2 M Na<sub>2</sub>SO<sub>4</sub> as an inert electrolyte. The size of the symbols represents the statistical error of the fitting process.<sup>43</sup> The rate constant

(41) Lelievre, D.; Plichon, V.; Laviron, E. *J. Electroanal. Chem.* **1980**, *112*, 137–145.

(42) Equation 2 can be written in the form

$$Y = \frac{KC_{dl}}{a} \frac{1}{\sqrt{\left[1 - \omega^2 \frac{R_s C_{dl}}{2k_{ct}}\right]^2 + \omega^2 \left[\frac{1}{2k_{ct}} + R_s C_{dl} \left(1 + \frac{1}{a}\right)\right]^2}}$$

where  $a = C_{dl}/C_a$ . If  $a \gg 1$  (or  $R_s C_{dl}(1 + a^{-1}) \ll 1/2k_{ct}$ ) the form and position of the curve is determined by  $k_{ct}$  only, and changes in the proportionality factor  $K$  are compensated by equal changes in  $a$ . In all cases reported these conditions were valid.

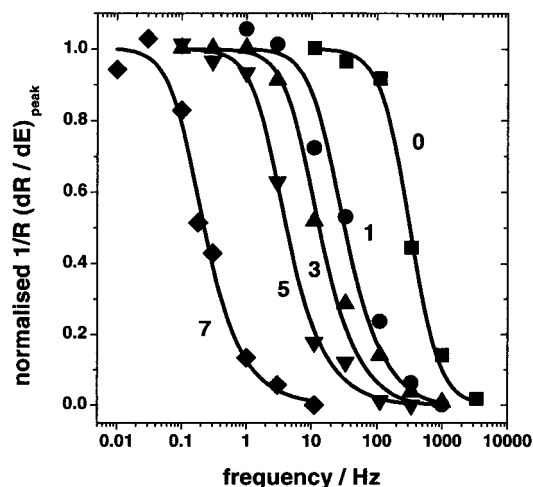


**Figure 5.** The electroreflectance response (measured at 600 nm in 0.2 M  $\text{Na}_2\text{SO}_4$ ) as a function of excitation frequency for type II multilayers with different number of insulating PDADMA and PSS layers (indicated in figure). All layers assembled from solutions containing 0.2 M  $\text{Na}_2\text{SO}_4$ . Experimental points and fitted curves are shown.

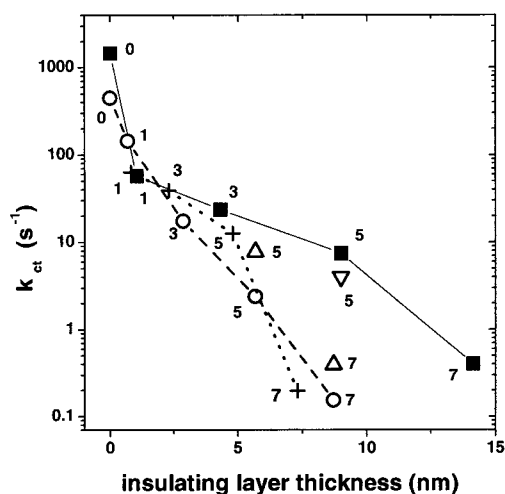


**Figure 6.** The charge-transfer rate constants calculated from the electroreflectance data for different type II multilayers as a function of the insulating layer thickness. PDADMA/PSS insulating layers: (■) all layers assembled in 0.2 M  $\text{Na}_2\text{SO}_4$ ; (○) all layers assembled in 0.02 M  $\text{Na}_2\text{SO}_4$ ; (△) insulating layers assembled in 0.02 M  $\text{Na}_2\text{SO}_4$ , P3TOPS in 0.2 M  $\text{Na}_2\text{SO}_4$ ; (▽) insulating layers assembled in 0.2 M  $\text{Na}_2\text{SO}_4$ , P3TOPS in 0.02 M  $\text{Na}_2\text{SO}_4$ . PXV/PSS insulating layers: (+) all layers assembled in 0.2 M  $\text{Na}_2\text{SO}_4$ . The number of insulating layers indicated for each point. All electroreflectance measurements carried out at 600 nm in aqueous 0.2 M  $\text{Na}_2\text{SO}_4$  solutions. The lines shown are only guides to the eye.

experiences a drop of ca. 4 orders of magnitude from  $1450 \text{ s}^{-1}$ , when P3TOPS is in direct contact with the electrode (the thickness of the underlying SAM is very small), to ca.  $0.40 \text{ s}^{-1}$  with seven insulating layers, before decreasing to zero with nine layers. The values obtained are similar to the charge-transfer rates observed with electroactive SAMs.<sup>39,40</sup>

The ionic strength of the adsorption solution is the major factor determining the thickness of the adsorbed polyelectrolyte layer.<sup>1,3,4</sup> If the PDADMA/PSS layers were adsorbed from 0.02 M  $\text{Na}_2\text{SO}_4$  solutions the insulating layers were considerably thinner. Figure 6 also displays the rate constants obtained when

all of the layers (including P3TOPS) have been adsorbed at this low ionic strength. Surprisingly, for three or more insulating layers the rate constants are lower than in the case of higher ionic strength (the value corresponding to the first point with zero separating layers may be considerably in error due to the minute amount of polyelectrolyte adsorbed). The curve falls clearly below the high ionic strength curve suggesting that the thinner PDADMA/PSS layers are better insulators than the thick layers (it should be noted that the thickness values in Figure 6 are operational ex situ values referring to the dried films, whereas polyelectrolyte multilayers are known to swell in solution). To clarify the role of the ionic strength we have carried out two additional measurements. First, the insulating PDADMA/PSS layers (and the capping PDADMA layer) were adsorbed from low ionic strength solutions containing 0.02 M  $\text{Na}_2\text{SO}_4$ , but P3TOPS was adsorbed from solutions of high ionic strength (0.2 M  $\text{Na}_2\text{SO}_4$ ). Second, PDADMA and PSS were adsorbed at high ionic strength, and P3TOPS, at low ionic strength. Interestingly, in the first case the rate constants increased exactly to the values corresponding to the same number of thick PDADMA/PSS layers. In the latter experiment the rate constant experienced a considerable drop from  $7.5$  to  $4.0 \text{ s}^{-1}$  although not reaching the value corresponding to the same number of thin insulating layers ( $2.4 \text{ s}^{-1}$ ). This behavior implies that the ionic strength of the solution used for the adsorption of a particular polyelectrolyte layer is more important for the interpenetration of this layer than the ionic strength of solutions used for the adsorption of the other layers (or their nominal thickness). In addition, the nature of the polyelectrolytes plays an important role. If P3TOPS is adsorbed on top of an insulating layer prepared from PXV and PSS (all adsorbed from 0.2 M  $\text{Na}_2\text{SO}_4$  solutions; PXV shows no redox conductivity at potentials used) the layers are thin, and the charge transfer rate constant drops off sharply (Figure 6). In all cases shown in Figure 6 no signal was observed when nine layers were inserted between P3TOPS and the electrode.

Polyelectrolyte layers close to the substrate surface differ somewhat from those further away and usually two to four bilayers are needed before a constant thickness increment *per* bilayer can be observed.<sup>44</sup> The insulating layers mainly represent so-called zones I and II of the whole polyelectrolyte multilayer as the thickness increased linearly after two to three bilayers for all insulating polyelectrolytes used in the present work.<sup>44</sup> The thickness increments were ca. 5.3 and 2.5 nm for the PDADMA/PSS and PXV/PSS bilayers assembled in 0.2 M  $\text{Na}_2\text{SO}_4$ , respectively, and ca. 3.4 nm for PDADMA/PSS bilayer assembled in 0.02 M  $\text{Na}_2\text{SO}_4$ . These values are similar to those reported previously for PDADMA/PSS multilayers.<sup>7</sup> The PXV/PSS layers were thinner than reported for the PBV/PSS system, which may be attributed to the more rigid nature of the PXV chains consisting of flat aromatic moieties.<sup>16a</sup> Electron transfer is a short-distance interaction decaying exponentially with the separation between the donor and acceptor. The decay constant is dependent on whether the transfer takes place through space or through bonds but is generally of the order of  $0.85\text{--}1.5 \text{ \AA}^{-1}$ .<sup>45</sup> In type II multilayers, a significant drop in the rate constant takes place already after insertion of one inactive layer (0.7–1 nm). This drop is, however, much smaller than expected on the

(44) Ladam, G.; Schaad, P.; Voegel, J. C.; Schaaf, P.; Decher, G.; Cuisinier, F. *Langmuir* **2000**, *16*, 1249–1255.

(45) (a) Li, T. T.-T.; Weaver, M. J. *J. Am. Chem. Soc.* **1984**, *106*, 6107–6108. (b) Closs, G. L.; Miller, J. R. *Science* **1988**, *240*, 440–447. (c) Moser, C. C.; Keske, J. M.; Warncke, K.; Farid, R. S.; Dutton, P. L. *Nature* **1992**, *355*, 796–802. (d) Finklea, H. O.; Hanshew, D. D. *J. Am. Chem. Soc.* **1992**, *114*, 3173–3181. (e) Slowinski, K.; Chamberlain, R. V.; Miller, C. J.; Majda, M. *J. Am. Chem. Soc.* **1997**, *119*, 11910–11919.

(43) Clifford, A. A. *Multivariate Error Analysis*; Applied Science Publishers Ltd.: London, 1973; p 30.

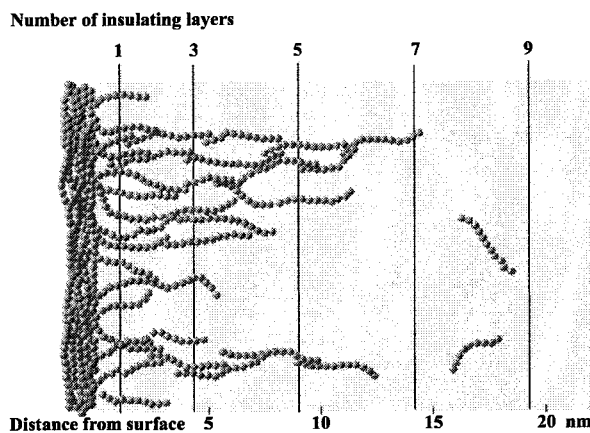


**Figure 7.** Penetration of P3TOPS into the insulating polyelectrolyte film. The position of the gold electrode surface is shown by vertical lines for different number of insulating dry PDADMA/PSS layers (assembled in 0.2 M Na<sub>2</sub>SO<sub>4</sub>, thickness of the MESA layer neglected). P3TOPS shown as a chain of balls; no indication of the number of monomer units per chain is included in this schematic figure.

basis of the distance dependence of electron transfer, and tunneling across the insulating layers cannot explain the charge transport. Therefore, as suggested earlier, the charge-transfer rate can be regarded as a measure of the interpenetration of the P3TOPS layer toward the electrode surface. The physical picture of the multilayer born out from these considerations is an insulator/conductor blend formed by the incoming conducting polyelectrolyte as it penetrates into the film (Figure 7). The constitution of the blend changes from a pure conductor at the top of the film to a pure insulator on the surface of the electrode with about nine or more insulating layers. Approximately eight outermost layers (excluding the capping PDADMA) are above the conduction percolation threshold and those closer to the substrate below it. We cannot exclude the presence of some isolated P3TOPS chains in latter deep-lying layers. The large effect of one insulating layer between the surface and P3TOPS suggests that intervening layers may cause a marked loss of electrical contact between the conducting layers in the bulk of the film also. This can explain the large increase of the conductivity in the all-thiophene multilayers, compared to PDADMA/P3TOPS films.

On the depth scale the extent of P3TOPS interpenetration varied from ca. 7 to 15 nm. The smallest interpenetration was found with PXV/PSS insulating layers assembled in 0.2 M Na<sub>2</sub>SO<sub>4</sub>, while the largest value corresponds to PDADMA/PSS layers prepared under the same conditions, the PDADMA/PSS layers adsorbed at low ionic strength being close to the former case. This is equivalent to seven to eight individual layers in all cases. These results are well in accordance with the previously reported data on the layer interpenetration.<sup>2a,4,8,10,16a</sup> There does not seem to be much difference between the unsymmetrical penetration of the outermost layer toward the substrate surface and the symmetrical interpenetration of a layer within the bulk of the film. The role of the ionic strength is interesting. While most of the previous work has been carried out using high ionic strength solutions for the polyelectrolyte adsorption the results at low ionic strength are surprisingly similar in terms of the number of interpenetrated layers (this work and ref 10). As to the effect of the ionic strength the experiments in which the small electrolyte concentration was different during the adsorption of insulating layers and the P3TOPS layer are specially informative. The ionic strength during the P3TOPS adsorption seems to be crucial, being able

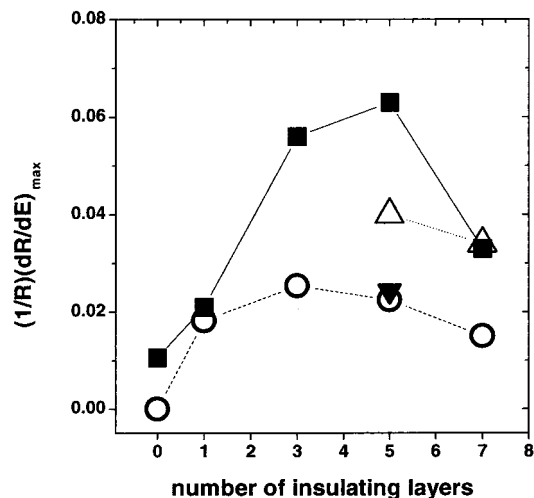


**Figure 8.** The maximum electroreflectance signal in type II multilayers with PDADMA/PSS insulating layers. Symbols: (■) all layers assembled at high ionic strength (0.2 M Na<sub>2</sub>SO<sub>4</sub>); (○) all layers assembled at low ionic strength (0.02 M Na<sub>2</sub>SO<sub>4</sub>); (△) P3TOPS at high and other layers at low ionic strength; (▼) P3TOPS at low and other layers at high ionic strength. Lines are shown as a guide to the eye.

to divert, either totally or to a large extent, the effect of the ionic strength used in the assembly of the previous layers. This phenomenon can be attributed to the reversible swelling of the bulk of the polyelectrolyte multilayers upon exposure to a higher ionic strength.<sup>44,46</sup> When a thin insulating multilayer prepared at low ionic strength is exposed to a P3TOPS solution containing 0.2 M Na<sub>2</sub>SO<sub>4</sub>, the ionic bonds within the PEM are broken, thus enabling the polythiophene chains to better penetrate into the film. On the other hand, the porous bulk of the PDADMA/PSS multilayer formed at high ionic strength contracts upon exposure to a P3TOPS solution containing 0.02 M Na<sub>2</sub>SO<sub>4</sub>. Therefore, the incoming polyelectrolyte “sees” the preformed layers in a state largely dictated by the ionic strength of the solution of that particular polyelectrolyte. This also implies that the solvation of the polyelectrolyte multilayer is an important factor in determining the layer interpenetration. This might explain the well-insulating nature of the thin PXV/PSS layers containing the more hydrophobic PXV chains.

The electroreflectance data can also be used to estimate the relative amount of electroactive material adsorbed. For each type II multilayer the maximum electroreflectance signal at the low-frequency limit is proportional to the amount of P3TOPS adsorbed (Figure 8). As expected, more P3TOPS was adsorbed from 0.2 M Na<sub>2</sub>SO<sub>4</sub> solutions than from solutions with low ionic strength. In both cases, the relative amount of adsorbed polythiophene increases with increasing number of insulator layers on the substrate surface before leveling off after about three layers. In polyelectrolyte multilayers, the amount of a polyelectrolyte adsorbed per layer is known to increase in the zone I close to the substrate surface.<sup>4,44</sup> The apparent decrease in the amount of adsorbed P3TOPS after four or more insulating prelayers is more puzzling. We tentatively attribute this to the formation of separate “arms” of P3TOPS reaching from the film surface toward the electrode. Close to the break of the electronic connection between the electrode and P3TOPS (i.e., with more than two PDADMA/PSS bilayers) the connection takes place only via few such arms while others represent dead ends (Figure 7). The coupling time constant between these two types of arms

(46) (a) Ödberg, L.; Sandberg, S.; Welin-Klintström, S.; Arwin, H. *Langmuir* **1995**, *11*, 2621–2625. (b) Sukhorukov, G. B.; Schmitt, J.; Decher, G. *Ber. Bunsen-Ges. Phys. Chem.* **1996**, *100*, 948–953.



may then become too large and the latter remain untouched by the ac excitation. The apparent amount of P3TOPS increases, relative to adsorption at low ionic strength, when the ionic strength of the P3TOPS solution was increased. The opposite behavior was observed if polythiophene was adsorbed at low ionic strength on a film formed at high Na<sub>2</sub>SO<sub>4</sub> concentration. These observations are in accordance with the ionic strength-dependent permeability of the insulating polyelectrolyte layer.

### Conclusions

Polyelectrolyte multilayers containing water-soluble electrically conducting polythiophene derivatives, poly-3-(3'-thienyloxy)propanesulfonate (P3TOPS) and poly-3-(3'-thienyloxy)propyltriethylammonium (P3TOPA), have been prepared and characterized. The electrochemical and optical behavior of these multilayers (type I films) in aqueous solution was similar to that of polythiophene films in organic media. The in-plane electrical conductivity of a P3TOPS/PDADMA multilayer was rather low, but it could be markedly increased by substituting a cationic polythiophene derivative P3TOPA for PDADMA, creating an all-thiophene multilayer. The charge-transfer rate between P3TOPS and the electrode surface was measured using modulated electroreflectance. The charge-transfer experienced a marked attenuation when insulating polyelectrolyte layers were inserted between the conducting layer and the electrode (type II films). This attenuation was attributed to the formation of an interpenetrating conducting network extending from the film outer surface toward the electrode. As the insulating layer thickness was increased, the number of arms reaching the substrate decreased. Therefore, the charge-transfer rate gives

information about the interpenetration of the incoming P3TOPS into the insulating polyelectrolyte multilayer. The extent of interpenetration is influenced by the nature of the insulating layers and depends critically on the ionic strength of the solution used for the adsorption of P3TOPS, that is, the interpenetrating polyelectrolyte. The insulating layer thickness required for complete break of the electric connection varied from ca. 7 to 15 nm, being in all cases, however, equivalent to eight to nine polyelectrolyte layers. These values are in accordance with literature data obtained with flexible polyelectrolytes. Therefore, although the length scale of interpenetration can be affected by the nature of the preformed multilayer, the results imply that the rigidity of the incoming polyelectrolyte does not greatly influence the interpenetration of that particular component.

**Acknowledgment.** The financial aid from the Academy of Finland (Grant No. 30579) and Turku University Foundation (N.K.) is gratefully acknowledged. We also thank Ms. Taina Laiho for the AFM measurements, Mr. Paul Ek (Åbo Akademi University, Turku) and Mr. Jukka Hellman (Turku Centre for Biotechnology) for the work with ICP-M.S. and MALDI-TOF, respectively.

**Supporting Information Available:** Raman spectra of P3TOPS and P3TOPA in water, table of the major band assignments, UV-vis spectra of the same polymers in water and DMSO, 400 MHz <sup>1</sup>H NMR and <sup>13</sup>C NMR spectra of the thiophene monomers (PDF). This material is available free of charge via the Internet at <http://pubs.acs.org>.

JA0043486